Journal of Solid State Chemistry **165,** 312–316 (2002)
doi:10.1006/jssc.2002.9535, available online at http://www.idealibrary.com on IDEAL®

Synthesis and Electrochemical Studies of Spinel $LiNi_{1-x}Mn_xVO_4$

Qiong Yu Lai,*[,1] Ji Zheng Lu,* Xiao Bo Su,* and Xiao Yang Ji†

*Chemical College of Sichuan University, Chengdu, 610064, China; and †Analytical and Testing Center of Sichuan University, Chengdu, 610064, China

Received August 29, 2001; in revised form January 30, 2002; accepted February 8, 2002

Spinel compound $LiNi_{1-x}Mn_xVO_4$ ($0 \le x \le 0.4$) had been prepared by using the moist chemical method. X-ray diffraction spectra showed that the lattice constant increased with x in the $LiNi_{1-x}Mn_xVO_4$, XPS spectra indicating that Li1*s* had a chemical shift towards lesser binding energy, and manganese in $LiNi_{1-x}Mn_xVO_4$ existing as the mixed valence of Mn^{2+} and Mn^{3+}. The electrochemical charge and discharge testing at a current density of 0.1 mA/cm^2 between the potentials of 4.0 and 3.0 V vs Li/Li$^+$ in 1 mol/dm^3 $LiPF_6$/EC+DEC (1:1 by volume) at 25°C showed that $LiNi_{1-x}Mn_xVO_4$ cell has a better rechargeability, but a lower cell voltage of 4.0 V vs Li/Li$^+$ than that without the doping sample, and the capacity and the cycle efficiency of the Li/$LiNi_{1-x}Mn_xVO_4$ cells increased with x in the $LiNi_{1-x}Mn_xVO_4$. © 2002 Elsevier Science (USA)

Key Words: **lithium–nickel–manganese–vanadate; inverse spinel; substitution; moist chemical method; synthesis; electrochemical characteristic.**

1. INTRODUCTION

In recent years, inverse spinel vanadates such as $LiNiVO_4$ and $LiCoVO_4$ as new systems of cathode materials for secondary lithium batteries have been reported because of their high voltage up to 4.8 V (vs Li) for Li/$LiNiVO_4$ cell and approximately 4.2 V (vs Li) for Li/$LiCoVO_4$ cell (1, 2). It had been proved that about 0.6 Li per formula unit could be extracted from the high-pressure spinel-phase $LiMnVO_4$ at about 3.8 V (vs Li) (3). According to the literature (3, 4), spinel LiMVO$_4$ (M = Ni, Co, Mn) is a cubic crystal, all the atoms in the inverse spinel structure occupy a special position in space group $Fd3m$, both Li and M (M = Ni, Co, Mn) occupying the octahedral sites (16*d*, $\frac{1}{2}$, $\frac{1}{2}$, $\frac{1}{2}$), vanadium in the tetrahedral sites (8*a*, $\frac{1}{4}$, $\frac{1}{4}$, $\frac{1}{4}$) and oxygen (32*e*, x, x, x), which can be expressed as $[V]_{tet}[Li, M]_{oct}O_4$ (M = Ni, Co, Mn). The partial substitution of M in the octahedral sites by another transition metal may have an effect on its structure and electrochemical property. The synthesis for this type of spinel can be achieved by the conventional solid-state reaction (5, 6) and a hydrothermal method (7). In this paper, using the moist chemical method, we synthesized inverse spinel $LiNi_{1-x}Mn_xVO_4$ ($0 \le x \le 0.4$) in which nickel was partially substituted by manganese. The products have been examined by X-ray diffraction (XRD), infrared spectroscopy (IR), X-ray photoelectron spectroscopy (XPS) and chemical analysis. The effect of product structure changing due to doping on its electrochemical characteristic will be discussed.

[1]To whom correspondence should be addressed. E-mail: laiqy@sc.homeway.com.cn.

2. EXPERIMENTAL PROCEDURE

2.1. Preparation of $LiNi_{1-x}Mn_xVO_4$

The reagent grade powders $LiOH \cdot H_2O$, $Ni(NO_3)_2 \cdot 6H_2O$, $Mn(CH_3COO)_2 \cdot 4H_2O$, and NH_4VO_3 were accurately weighted by a molar ratio of Li:Ni:Mn:V = $1:(1-x):x:1$ (x = 0, 0.1, 0.2, 0.3, 0.4, 0.5) and were mixed in an agate mortar, in which adding the moderate distilled water and ethanol solution (95%), the above mixture was dissolved under grinding. The xerogel was gained by driving away solvents at 70–80°C on the steamer. The xerogel used as the precursor was sintered at 550–850°C for 4–8 h and the series of products could be obtained after cooling gradually.

2.2. Analysis of Products

The phases and the crystal structure of products were determined by X-ray diffraction analysis (XRD), an X-ray diffractionmeter, Japan D/max-rA was used, Cu$K\alpha$ line, 40 kv, 150 mA and λ = 0.15405 nm. The IR spectra of the samples were tested by PE 16F-IR apparatus in the wavenumber range of 400–4000 cm^{-1}. The XPS data were obtained with a Britain Kratos XSAM 800 photoelectron spectrometer, and the binding energy was calibrated with reference to the C1*s* level of carbon (284.8 ev). The determination of chemical composition for $LiNi_{1-x}Mn_xVO_4$ was carried out by chemical analysis.

0022-4596/02 $35.00

TABLE 1
The Reaction Conditions and the Resulting Products for Preparation of $LiNi_{1-x}Mn_xVO_4$

Sample	Li:Ni:Mn:V Ratio	Reaction Temp. (°C)	Reaction Time (h)	Products analyzed by XRD
1	1:1:0:1	550	6	$LiNiVO_4$
2	1:0.9:0.1:1	750	4	$LiNi_{0.9}Mn_{0.1}VO_4$
3	1:0.8:0.2:1	750	4	$LiNi_{0.8}Mn_{0.2}VO_4$
4	1:0.7:0.3:1	750	4	$LiNi_{0.7}Mn_{0.3}VO_4$
5	1:0.6:0.4:1	750	4 + 3[a]	$LiNi_{0.6}Mn_{0.4}VO_4$
6	1:0.5:0.5:1	850	4 + 4[a]	$LiNi_{1-x}Mn_xVO_4$ + $LiVO_3$ + Mn_2O_3

[a]First sintered for 4 h, then at the same temperature for 3 or 4 h after being ground.

2.3. Electorchemical Measurements

The charge and discharge tests were carried out on PCBT-138-8D-A instrument by adopting CR2032 coin cells in which $LiNi_{1-x}Mn_xVO_4$ ($0 \le x \le 0.4$) and Li metal foil were used as the cathode materials and anodes, respectively, celgard 2400 microporous polypropylene was used as the cell separators. The cathode was prepared from a mixture of $LiNi_{1-x}Mn_xVO_4$ ($0 \le X \le 0.4$, 80% by weight), acetylene black (15% by weight) and Teflon binder (5% by weight). The electrolyte solution (Japan Mitsubishi Chemical Co.) was 1 mol/dm^3 $LiPF_6$ dissolved in a mixture solvent which consisted of ethylene carbonate (EC) and diethylene carbonate (DEC) in a volume percent of 1:1.

3. RESULTS AND DISCUSSION

3.1. XRD Analysis

Table 1 gives the reaction conditions and the resulting products analyzed by XRD for preparing $LiNi_{1-x}Mn_xVO_4$ ($0 \le x \le 0.5$). From the table, it is clear that the product of $x = 0$ in $LiNi_{1-x}Mn_xVO_4$ could be obtained when the xerogel was heated at 550°C for 6 h (see sample no.1). Those products using manganese as a substitute for nickel, namely single phases $LiNi_{1-x}Mn_xVO_4$ ($x = 0.1, 0.2, 0.3, 0.4$), could easily be obtained by sintering the xerogel at 750°C for 4 h (see samples nos. 2–5) except the $LiNi_{0.6}Mn_{0.4}VO_4$ which spent more reaction time of 7 h to be gained. It is difficult to obtain the single-phase $LiNi_{0.5}Mn_{0.5}VO_4$ although the xerogel was sintered at a higher reaction temperature of 850°C and for more reaction time of 8 h (no. 6), but only getting the mixed phases including spinel $LiNi_{1-x}Mn_xVO_4$, $LiVO_3$, and Mn_2O_3. According to the above results, we reasonably consider that the amounts of replacing nickel by manganese are limited, a tolerable range is of $0 \le x \le 0.4$ in $LiNi_{1-x}Mn_xVO_4$. The XRD spectrum of $LiNiVO_4$ without manganese is shown in Fig. 1a. Although we obtained all the

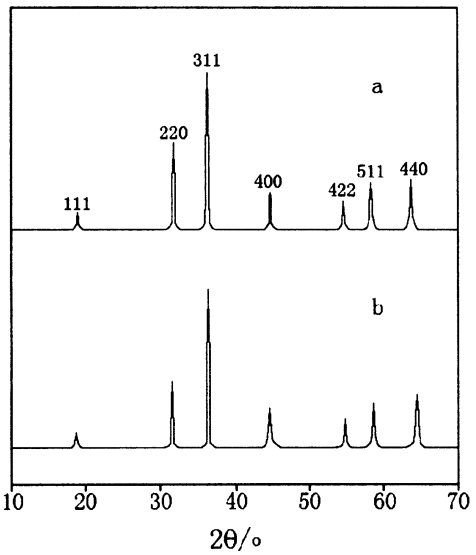

FIG. 1. XRD spectra for $LiNi_{1-x}Mn_xVO_4$. (a) $x = 0$ and (b) $x = 0.4$.

XRD spectra of $LiNi_{1-x}Mn_xVO_4$ ($x = 0.1, 0.2, 0.3, 0.4$), the XRD spectrum of $LiNi_{0.6}Mn_{0.4}VO_4$ is only present which is displayed in Fig. 1b. The X-ray diffraction data for $LiNi_{1-x}Mn_xVO_4$ ($x = 0$, 0.1, 0.2, 0.3, 0.4) are as shown in Table 2 in which the cubic lattice constant a of $LiNi_{1-x}Mn_xVO_4$ can be gained by using the formula $a = d(h^2 + k^2 + l^2)^{1/2}$ according to the all the Bragg peaks in the range of 10–70 degrees. In the formula "d" is the distance between vicinal crystal face and hkl is the Miller index. $LiNi_{1-x}Mn_xVO_4$ ($x = 0.1, 0.2, 0.3, 0.4$) have an XRD spectra analogous $LiNiVO_4$, but all the products have the different lattice constants from each other which is the reason for change in the scattering angle with x in $LiNi_{1-x}Mn_xVO_4$. The crystal structure of $LiNi_{1-x}Mn_x$

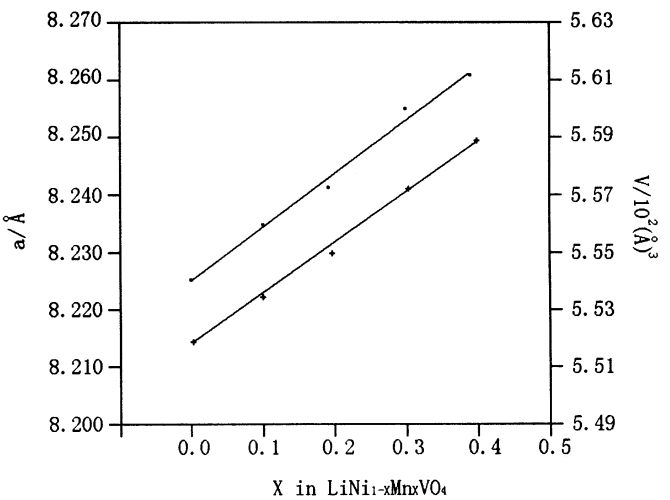

FIG. 2. The lattice constants and the volumes of crystal cell for $LiNi_{1-x}Mn_xVO_4$. v (■); a (+).

TABLE 2
X-Ray Diffraction Data for $LiNi_{1-x}Mn_xVO_4$

x value in $LiNi_{1-x}Mn_xVO_4$			$x = 0$		$x = 0.1$		$x = 0.2$		$x = 0.3$		$x = 0.4$	
Unit cell a/Å			8.215		8.222		8.229		8.241		8.250	
Cell volume v/Å^3			554.4		555.8		557.2		559.7		561.5	
h	k	l	d_{obs}	d_{cal}	d_{obs}	d_{cal}	d_{obs}	d_{cal}	d_{obs}	d_{cal}	d_{obs}	d_{cal}
1	1	1	4.740	4.743	4.743	4.747	4.746	4.751	4.750	4.758	4.754	4.763
2	2	0	2.904	2.904	2.906	2.907	2.909	2.909	2.914	2.914	2.918	2.917
3	1	1	2.479	2.477	2.480	2.479	2.482	2.481	2.486	2.485	2.488	2.487
4	0	0	2.056	2.054	2.057	2.056	2.061	2.057	2.062	2.060	2.064	2.063
4	2	2	1.676	1.677	1.679	1.678	1.680	1.680	1.683	1.682	1.684	1.684
5	1	1	1.581	1.581	1.582	1.582	1.583	1.584	1.586	1.586	1.589	1.588
4	4	0	1.452	1.452	1.453	1.453	1.454	1.455	1.456	1.457	1.458	1.458

VO_4 was determined to be a cubic lattice having a space group $Fd3m$ in which lithium, nickel and manganese ions are at 16(d) sites, vanadium at 8(a) sites and oxygen at 32(e) sites. The lattice constants and crystal cell volume increased with the molar amounts of manganese doped in $LiNi_{1-x}Mn_xVO_4$ as shown in Fig. 2. Because the ionic radii of Mn^{2+} is larger than that of Ni^{2+} in the tetrahedral sites [8], the volume increase should be related to manganese substituting for nickel.

3.2. IR Results

The IR spectrum in the wavenumber range of 400–4000 cm^{-1} for $LiNi_{0.6}Mn_{0.4}VO_4$ is represented in Fig. 3a, which was analogous to the spectrum of undoped sample as Fig. 3b; there was a broad strong absorption band in the 450–850 cm^{-1} region. This absorption band could be assigned to the stretching vibrations of VO_4 tetrahedrons (9). Both spectra are clearly different from the IR spectrum of V_2O_5 as seen in Fig. 3c. This fact indicates that $LiNi_{1-x}Mn_xVO_4$ has a similar structure of vanadates as that of $LiNiVO_4$, and the conclusion agrees with the result from XRD analysis. It is clearly observable that there are some small splitting peaks, such as four peaks in Fig. 3a and three peaks in Fig. 3b. The detailed frequency values are listed in Table 3. We can observe small shifts toward low wavenumbers in V–O frequencies from the IR spectrum of $LiNiVO_4$ to that of $LiNi_{0.6}Mn_{0.4}VO_4$. The shift phenomenon can be tentatively considered as being the cause of manganese substituting for nickel. The splitting peaks in both IR spectra in this region can be explained by the fact that the VO_4 tetrahedron may be bonded to two or three types of cations and this makes the symmetrization in the VO_4 tetrahedron lower. As seen in this figure, a weak peak located at 1120 cm^{-1} in Fig. 3b belonged to the Ni–O stretching vibration absorption peak which became of a smaller peak as shown in Fig. 3a. This result probably is caused by using manganese as a substitute for nickel.

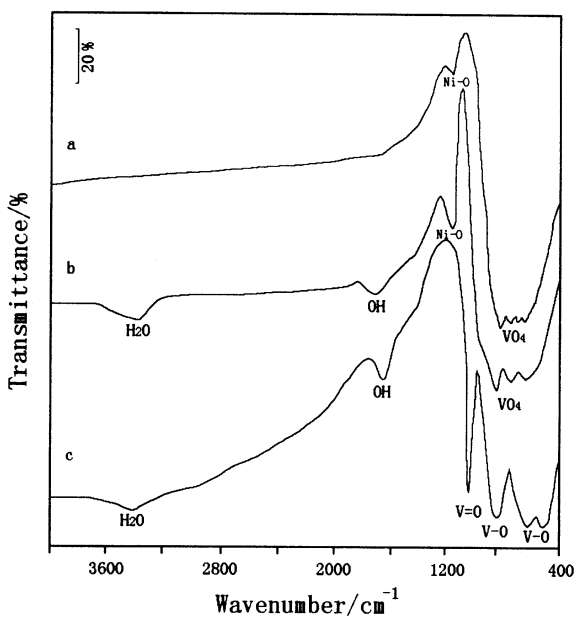

FIG. 3. IR spectra for the samples (a) $LiNi_{0.6}Mn_{0.4}VO_4$, (b) $LiNiVO_4$, and (c) V_2O_5.

TABLE 3
The Frequencies of $LiNi_{1-x}Mn_xVO_4$

	Wavenumber (cm^{-1})	
Peaks	$LiNiVO_4$	$LiNi_{0.6}Mn_{0.4}VO_4$
1	810	801
2	720	717
3		667
4	644	632

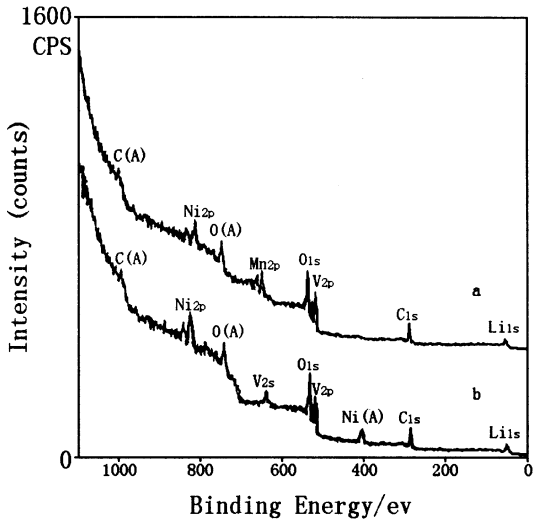

FIG. 4. Widescan XPS spectra of $LiNi_{1-x}Mn_xVO_4$: (a) $x = 0.4$ and (b) $x = 0$.

3.3. XPS Analysis

A widescan XPS spectra of $LiNi_{1-x}Mn_xVO_4$ are shown in Fig. 4a for $x = 0.4$ and (b) for $x = 0$, respectively, which reveal a series of peaks arising from the direct excitation of electrons from core levels. Those peaks of Li1*s*, Ni2*p*, V2*p*, O1*s* and the peak of C1*s* were used as a reference peak of 284.8 ev in both Fig. 4a and b. In addition to surface core level lines X-ray-induced Auger electron peaks of O (A) and C (A) are also observed. The fact that the widescan XPS spectrum of $LiNi_{1-x}Mn_xVO_4$ (Fig. 4a) is somewhat similar to that of $LiNiVO_4$ (Fig. 4b) except that Mn2*p* peak appeared in Fig. 4a due to doping, has been noticed. The product $LiNi_{0.6}Mn_{0.4}VO_4$ gave $Mn2p_{1/2}$ and $Mn2p_{3/2}$ peaks at the binding energies of 653.9 and 642.1 eV, respectively, as seen in Fig. 5. Therefore, it can be assumed that the

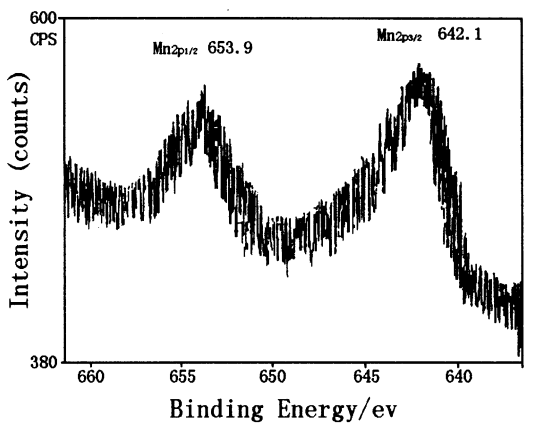

FIG. 5. Mn2*p* XPS spectrum of $LiNi_{0.6}Mn_{0.4}VO_4$.

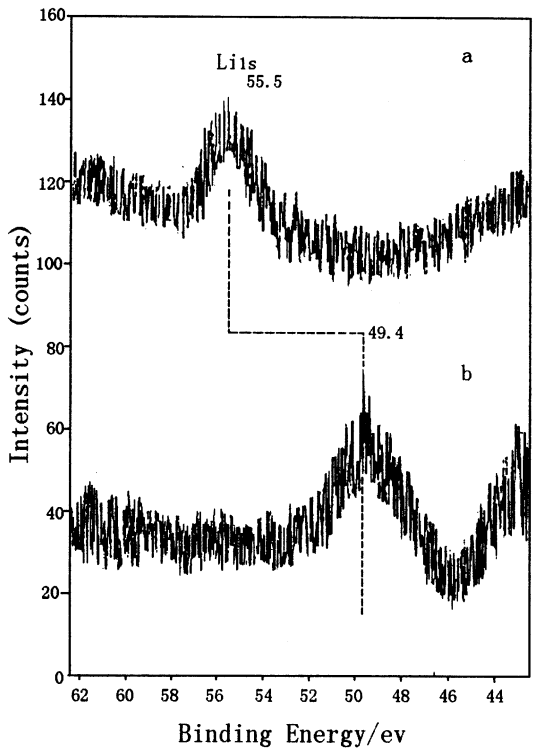

FIG. 6. Li_{1s} XPS spectra of $LiNi_{1-x}Mn_xVO_4$. (a) $x = 0$ and (b) $x = 0.4$.

manganese in the $LiNi_{0.6}Mn_{0.4}VO_4$ exists as the mixed valence of Mn^{2+} and Mn^{3+}. The chemical shift arising from doping manganese has been exhibited in Li1*s* spectra of the product $LiNi_{1-x}Mn_xVO_4$, which are shown in Fig. 6. The Li1*s* of $LiNiVO_4$ shifted from 55.5 eV (Fig. 6a) down to 49.4 eV (Fig. 6b) after forming

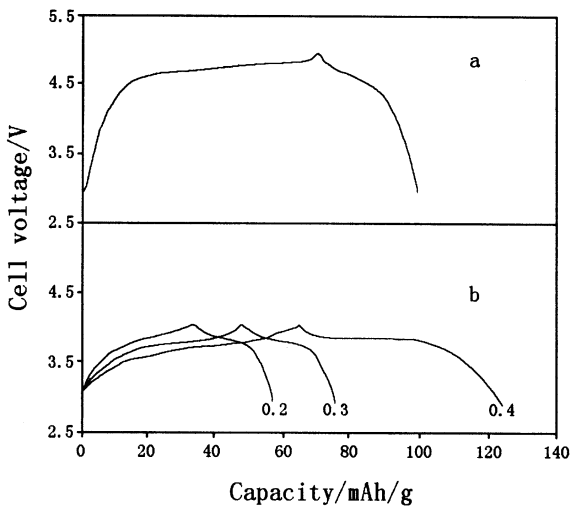

FIG. 7. First charge and discharge curves for $Li/LiNi_{1-x}Mn_xVO_4$ cells with a current density of 0.1 mA/cm^2 at 25°C: (a) $x = 0$ and (b) $x = 0.2$, 0.3, 0.4.

TABLE 4
The Element Contents of $LiNi_{1-x}Mn_xVO_4$

Target materials	Content values (wt %)				Results
	Li	Mn	Ni	V	
$LiNiVO_4$	3.76	0	32.60	28.28	$Li_{0.976}Ni_{1.000}V_{1.000}O_4$
$LiNi_{0.8}Mn_{0.2}VO_4$	3.70	6.21	26.22	28.34	$Li_{0.959}Ni_{0.802}Mn_{0.203}V_{1.000}O_4$
$LiNi_{0.7}Mn_{0.3}VO_4$	3.68	9.29	23.10	28.41	$Li_{0.951}Ni_{0.705}Mn_{0.303}V_{1.000}O_4$
$LiNi_{0.6}Mn_{0.4}VO_4$	3.65	12.23	19.72	28.48	$Li_{0.941}Ni_{0.601}Mn_{0.398}V_{1.000}O_4$

$LiNi_{0.6}Mn_{0.4}VO_4$. A possible explanation for the above phenomenon is that Li^+–O^{2-} bonds were weakened because of Mn^{3+}–O^{2-} bonds being stronger than Ni^{2+}–O^{2-} bonds in Li–O–M bonds (M = Ni, Mn) existing in the octahedron sites.

3.4. Chemical Composition Determination

The measured results of $LiNi_{1-x}Mn_xVO_4$ are described in Table 4. It is indicated that the stoichiometries of nickel, vanadium and substituent manganese in all the results correspond well with that in the relevant target materials, but only lithium being somewhat deficient and maybe partly existing vacant in the lithium sites. According to the results of chemical composition determination and the result of XRD analysis and XPS analysis, the $LiNi_{1-x}Mn_xVO_4$ can be further expressed as the following formula:

$$Li_{1-y}(V_{Li})_yNi_{1-x}Mn(III)_yMn(II)_{x-y}VO_4 \ (x > y > 0).$$

In the above formula V_{Li} is lithium vacancy. This formula illustrates that the additional y positive charge caused by yMn^{3+} substituting for yNi^{2+} can be compensated by the formation of yV_{Li} due to removal of y lithium.

3.5. Electrochemical Characteristics

Figure 7 shows the first charge and discharge curves for $Li/LiNi_{1-x}Mn_xVO_4$ cells with a current density of 0.1 mA/cm^2 at 25°C. The cutoff voltages were 4.8 V for charge and 3.0 V for discharge when $x = 0$ in $LiNi_{1-x}Mn_xVO_4$ as seen in Fig. 7a. About 70 mAh/g of capacity is obtained during the first charge to 4.8 V, however, only 30 mAh/g of capacity could be gained during the first discharge to 3.0 V. This process yielded a cycle efficiency of 43%. The charge, discharge capacities and the cycle efficiency of $Li/LiNi_{1-x}Mn_xVO_4$ cells between 4.0 and 3.0 V increased with the amount of manganese doped in $LiNi_{1-x}Mn_xVO_4$ shown in Fig. 7b. The cycle efficiency of 78, 85 and 92% for $x = 0.2$, 0.3 and 0.4 samples in turn can be seen. The $Li/LiNi_{1-x}Mn_xVO_4$ cell exhibited a lower voltage of 4.0 V than $Li/LiNiVO_4$ cell which had the cell voltage of up to 4.8 V, corresponding to the literature [1], shown in Fig. 7a. The possible explanation was that the expanding of lattice in manganese-doped samples was favored for Li^+ extracting and inserting. Another presumable interpretation was that the electrolyte had not been oxidized at the lower cell voltage of 4.0 V (vs Li); it would be helpful to improve the cell's cycle behaviors.

4. CONCLUSIONS

This paper has shown the substitution of nickel at octahedron sites in $LiNiVO_4$ by manganese. XRD, IR, XPS analyses showed that the doping over a suitable range of $0 \le x \le 0.4$ in $LiNi_{1-x}Mn_xVO_4$ did not change the spinel structure of $LiNiVO_4$, but the lattice constant increased with the doping amount of manganese. The $LiNi_{1-x}Mn_xVO_4$ can be further expressed as $Li_{1-y}(V_{Li})_yNi_{1-x}Mn(III)_yMn(II)_{x-y}VO_4$ ($x > y > 0$). The electrochemical measurement of $Li/LiNi_{1-x}Mn_xVO_4$ cells exhibited a lower cell voltage of 4.0 V, but improved the cycle efficiency with increasing x values in $LiNi_{0.6}Mn_{0.4}VO_4$ ($0 \le x \le 0.4$).

ACKNOWLEDGMENTS

We gratefully acknowledge the financial support for this work by the National Nature Science Foundation of China. We also thank Jiang Zhong Lithium Battery Factory for installing coin cells.

REFERENCES

1. George Ting-Kuo Fey, Wu Li, and J. R. Dahn, *J. Electrochem. Soc.* **141**(9), 2279 (1994).
2. George Ting-Kuo Fey and Chi-San Wu, *Pure Appl. Chem.* **69**(11), 2329 (1997).
3. A. K. Padhi, W. B. Archibald, K. S. Nanjundaswamy, *et al.*, *J. Solid State Chem.* **128,** 267 (1997).
4. C. Gonzalez, M. Gaitan, M. L. Lopez, *et al.*, *J. Mater. Sci.* **29,** 3456 (1994).
5. W. Wong-Ng, H. Mc Murdie, B. Partetzkin, *et al.*, JCPDS 38-1395.
6. George Ting-Kuo Fey and Way-Bing Perng, *Mater. Chem. Phys.* **47,** 279 (1997).
7. Chung Hsin Lu, Wei Cheng Lee, Shaw Jang Liou, *et al.*, *J. Power Sources* **81–82,** 696 (1999).
8. R. D. Shannon, *Acta Crystallogr. A* **32,** 751 (1976).
9. J. Preudhomme and P. Tarte, *Spectrochimica Acta A* **28,** 69 (1972).